JACS
JOURNAL OF THE AMERICAN CHEMICAL SOCIETY
Communication
pubs.acs.org/JACS

Protonation and Concerted Proton–Electron Transfer Reactivity of a Bis-Benzimidazolate Ligated [2Fe–2S] Model for Rieske Clusters

Caroline T. Saouma, Werner Kaminsky, and James M. Mayer*

Department of Chemistry, University of Washington, Box 351700, Seattle, Washington 98195-1700, United States

Supporting Information

ABSTRACT: A model system for biological Rieske clusters that incorporates bis-benzimidazolate ligands (^{Pr}bbim)$^{2-}$ has been developed (^{Pr}bbimH$_2$ = 4,4-bis-(benzimidazol-2-yl)heptane). The diferric and mixed-valence clusters have been prepared and characterized in both their protonated and deprotonated states. The thermochemistry of interconversions of these species has been measured, and the effect of protonation on the reduction potential is in good agreement to that observed in the biological systems. The mixed-valence and protonated congener [Fe$_2$S$_2$(^{Pr}bbim)(^{Pr}bbimH)](Et$_4$N)$_2$ (**4**) reacts rapidly with TEMPO or *p*-benzoquinones to generate diferric and deprotonated [Fe$_2$S$_2$(^{Pr}bbim)$_2$]-(Et$_4$N)$_2$ (**1**) and 1 equiv of TEMPOH or 0.5 equiv of *p*-benzohydroquinones, respectively. The reaction with TEMPO is the first well-defined example of concerted proton–electron transfer (CPET) at a synthetic ferric/ferrous [Fe–S] cluster.

Iron–sulfur clusters are ubiquitous electron-transfer (ET) cofactors and they play an integral role in many enzymes that catalyze multi-e$^-$/H$^+$ redox events.[1] In some cases, the [Fe–S] clusters are known to undergo proton-coupled electron transfer (PCET).[2] Biochemical and model studies are providing insight into the PCET reactivity of low-valent CO-ligated [Fe–S] clusters in hydrogenases,[3] but much less is known about the involvement of protons in the more widespread high-valent clusters.[2] The [2Fe–2S] Rieske cluster, in which one Fe is ligated by two Cys residues and the other by two His residues, is perhaps the best characterized biological [Fe–S] cluster that undergoes PCET.[2a,4] This PCET reactivity enables Rieske clusters to act as structural gates in oxygenase enzymes (reduction/protonation of the cluster induces structural changes that affect the active site),[5] and PCET is their primary function in the Q-cycle of the mitochondrial and photosynthetic electron transport chains.[4b,6] In the latter role, the diferric Rieske cluster accepts a net H-atom (e$^-$ + H$^+$) from a hydroquinone (H$_2$Q), reducing the cluster to the mixed-valence state and protonating the imidazolate (His) ligand. The mechanism of H$_2$Q oxidation by the Rieske cluster is a topic of debate, with both stepwise proton transfer/electron transfer (PT-ET) and concerted proton–electron transfers (CPET) having been invoked.[4b,7] This issue is important because the ET steps within the Q-cycle are tightly regulated to avoid energetically wasteful short-circuits and formation of reactive oxygen species.[6a,8]

Reported here are studies of the PCET reactivity of a model Rieske cluster, including the first example of CPET reactivity of a noncarbonyl [Fe–S] cluster.[3b] Four congeners of a family of bis-benzimidazolate ligated [2Fe–2S] clusters have been prepared and interconverted, thus defining the full PCET square scheme (**1**–**4**, Scheme 1). The protonated congeners are the first characterized examples of protonated high-valent [Fe–S] clusters.[9]

Scheme 1. Square Scheme for [Fe$_2$S$_2$(^{Pr}bbim)$_x$(^{Pr}bbimH)$_{2-x}$]$^{n-}$ Clusters

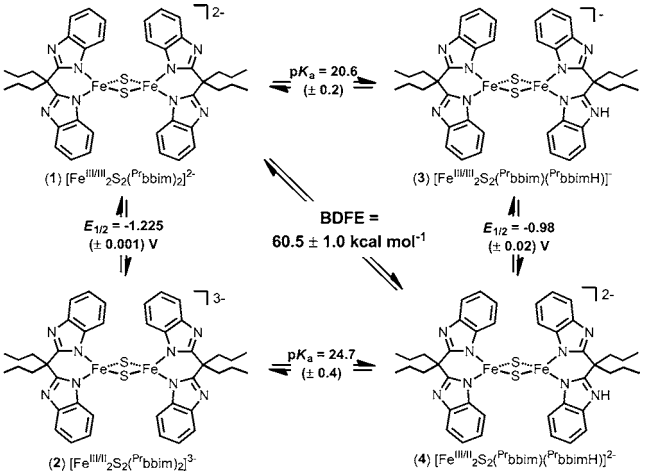

Diferric and mixed-valence bis-benzimidazolate ligated clusters were first prepared and characterized by Gibson (including **1** and **2**),[10] and recent detailed spectroscopic studies have been done by Franc Meyer and co-workers.[11] Diferric [Fe$^{III}_2$S$_2$(^{Pr}bbim)$_2$](Et$_4$N)$_2$ (**1**) and mixed-valence [Fe$^{III/II}_2$S$_2$(^{Pr}bbim)$_2$](Et$_4$N)$_3$ (**2**) are readily prepared by minor modification of the literature procedures.[10a] Clusters **1** and **2** comprise high-spin iron centers that are antiferromagnetically coupled to give S = 0 and S = 1/2 ground-states, respectively.[10b,c,11] ^{1}H NMR spectra of **1** and **2** each display 9 well-resolved resonances close to the diamagnetic region (δ 0.9–12.2 ppm; Figure 1a,c and Supporting Information (SI) Figures S2–S5), indicating D_{2h} symmetry in solution. The (^{Pr}bbim)$^{2-}$ to Et$_4$N$^+$ ratios of 1:1 for **1** and 2:3 for **2** confirm the stoichiometries. The latter spectrum also indicates valence delocalization on the NMR time scale for **2**.[10b]

Received: February 27, 2012
Published: April 21, 2012

dx.doi.org/10.1021/ja3019324 | J. Am. Chem. Soc. 2012, 134, 7293–7296

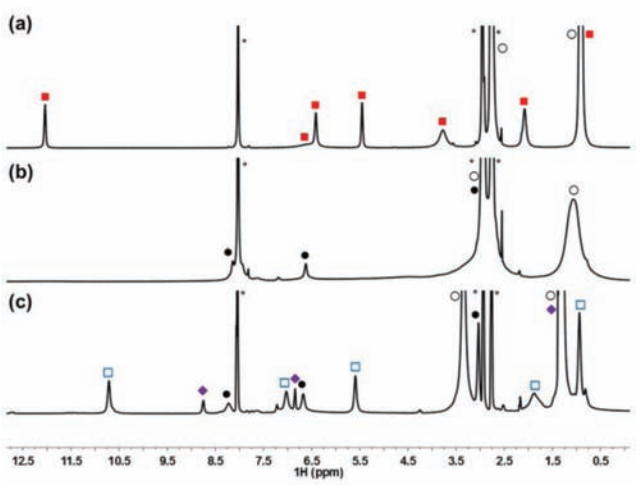

Figure 1. ^{1}H NMR spectra (d_7-DMF) of (a) mixed-valence **2** (−20 °C); (b) reaction of **2** with [DMAP-H]$^+$ to give mixed-valence and protonated **4** (−20 °C); (c) reaction of **4** with 0.5 equiv of ^{t}Bu$_2$Q to give **1** and 0.5 equiv of ^{t}Bu$_2$H$_2$Q. Legend: red ■ = 2; blue □ = 1; purple ◆ = ^{t}Bu$_2$H$_2$Q; ● = DMAP; ○ = Et$_4$N+; * = DMF.

The solid-state structures of both **1** and **2** have been obtained. The structures are very similar and that of **2** is shown in Figure 2. The metrical parameters of **1**, d(Fe−N$_{ave}$) = 1.978

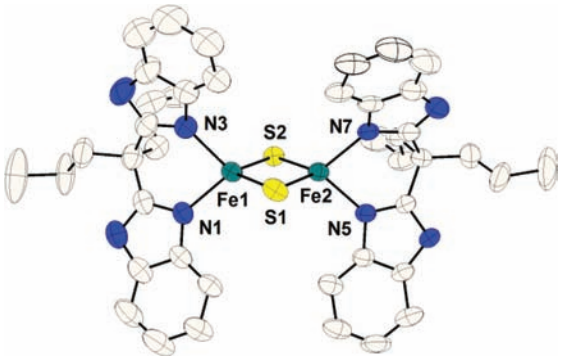

Figure 2. Thermal ellipsoid (50%) representation of mixed-valence cluster **2**. Hydrogen atoms, Et$_4$N$^+$, and minor components of disorder have been omitted for clarity; see the SI for details and metrical comparisons of **1** and **2**.

Å and d(Fe−S$_{ave}$) = 2.197 Å, are as expected for diferric clusters.[11,12] Upon reduction, the Fe−N$_{ave}$ and Fe−S$_{ave}$ bond distances elongate by ca. 0.07 and 0.03 Å, respectively. The iron centers in **2** are crystallographically unique (unlike the one other mixed-valence [2Fe−2S] structure[11]), with one iron having Fe−S$_{ave}$ and Fe−N$_{ave}$ distances that are statistically longer than the other. This is consistent with Mössbauer studies on related compounds, indicating that the valence may be partially localized in the crystal at 110 K.[10c,11]

Diferric **1** is converted to the protonated derivative **3** by 1 equiv of [pyH]OTf in MeCN. By analogy with the biological Rieske clusters, we tentatively assign the site of protonation as a benzimidazolate nitrogen, [Fe$^{III}_2$S$_2$(^{Pr}bbim)(^{Pr}bbimH)](Et$_4$N). The IR spectrum of **3** shows no discernible N−H or S−H stretch and there are no noticeable differences between the IR spectra of **3** and **3-D** (Figure S14).

When the protonation is monitored by optical spectroscopy, isosbestic points are observed with ≤1 equiv [pyH]OTf, and addition of DBU regenerates **1** (DBU = 1,8-diazabicycloundec-7-ene; Figure S11). Reversible protonation is observed by ^{1}H NMR spectroscopy as well. ^{1}H NMR spectra of **3** show a single set of ligand resonances, indicating that proton transfer among the four benzimidazolates is rapid on the NMR time scale (Figure S6). NMR spectra of mixtures of **1** and **3** also show a single set of ligand resonances that shift according to the ratio of **1** and **3**, indicating that intermolecular PT is fast between diferric clusters (Figure S7). No decoalescence of the resonances for **3** is observed upon cooling samples in CD_2Cl_2 (−70 °C), d_8-THF (−50 °C), d_7-DMF (−50 °C), or CD_3CN (−30 °C).

Complex **3** is unstable in MeCN solution, decomposing over the course of hours to ^{Pr}bbimH$_2$, **1**, and unidentified iron-containing species ($t_{1/2}$ ca. 4 h at 22 °C; 3.8 mM solution). The formation of both ^{Pr}bbimH$_2$ and **1** suggests that the decomposition involves a second protonation. Protonation has been previously shown to facilitate ligand exchange and decomposition in synthetic [Fe−S] clusters.[9b,12]

Mixed-valence **2** can likewise be protonated, with [DMAP-H]OTf or [pyH]OTf, to generate [Fe$^{III/II}_2$S$_2$(^{Pr}bbim)(^{Pr}bbimH)](Et$_4$N)$_2$ (**4**) (4-DMAP = 4-dimethylaminopyidine). Again, this protonation is reversible, with ^{1}H NMR spectra showing regeneration of **2** upon addition of the strong noncoordinating base ^{t}butylimino-tri(pyrrolidino)phosphorane (^{t}BuNP(pyrr)$_3$; Figure S9). Solutions of mixed-valence **4** in MeCN show no degradation over at least 30 min at −24 °C, but decompose at 22 °C with a $t_{1/2}$ of ca. 20 min. Complex **4** is thus less stable than diferric **3**. The decomposition products have not been identified, but their ^{1}H NMR spectra suggest formation of a monomeric iron(II) species (a similar species forms upon mixing FeCl$_2$ and ^{Pr}bbim$_2$Tl$_2$, Figure S25), indicating that the Fe$_2$S$_2$ core does not stay intact. NMR experiments show that **3** and **4** can be interconverted with [Cp$_2$Fe]PF$_6$ and Cp$_2$Co, although not without some decomposition.

Mixed-valence and protonated **4** has a solution magnetic moment of 2.4 μ_B in d_7-DMF at −25 °C. The EPR spectrum of **4** was obtained, and is shown in Figure 3a. The spectrum can be

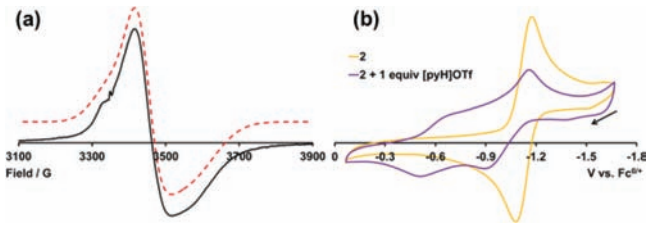

Figure 3. (a) X-band EPR spectrum of **4** collected at 120 K in a 2:3 MeCN/toluene glass (solid black) and the calculated fit (dotted red; displaced vertically from the experimental). (b) CVs of **2** in the absence (yellow) and presence (purple) of 1 equiv [pyH]OTf at −20 °C in 0.25 M [^{n}Bu$_4$N]PF$_6$ in MeCN, with scan-rates of 100 mV s^{-1}.

fit to a rhombic g tensor with g = [1.983, 1.943, 1.860] and corresponding linewidths W = [61, 22, 84 G]. For comparison, the EPR spectrum of **2** obtained under similar conditions has g = [2.012, 1.940, 1.835] and W = [40, 70, 145 G] (Figure S13). Thus, **4** has an S = 1/2 ground-state like **2**.

Protonated **4** is essentially NMR silent (Figures 1b and S8), in contrast to the sharp signals observed for **2**. Only resonances ascribed to the Et$_4$N$^+$ cations are readily observed within ±170 ppm, in both CD_3CN (−20 to 25 °C) and d_7-DMF (−50 to 25

dx.doi.org/10.1021/ja3019324 | J. Am. Chem. Soc. 2012, 134, 7293−7296

°C). NMR spectra of mixtures of **2** and **4** show a single set of resonances that is not shifted from that of **2** and integrate according to the mole fraction of **2** in solution (relative to the conjugate base or Et_4N^+). Thus, PT between **2** and **4** is slow on the NMR time scale, and the lack of an observable spectrum for **4** cannot be due to exchange with **2**. Most likely the larger NMR linewidths for **4** are due to a change in the electronic relaxation upon protonation of **2**.[13] The electronic relaxation of mixed-valence [2Fe−2S] clusters is dominated by an Orbach mechanism at these temperatures,[14] and hence, perturbation of the excited-state energies will affect NMR linewidths.

The ability to generate the protonated congeners **3** and **4** allows for the direct measurement of their pK_as. Solutions of diferric **3**, generated *in situ* from **1** and [pyH]OTf, were titrated with quinuclidine and monitored by optical spectroscopy. Using the quinuclidine pK_a of 19.51 in MeCN,[15] the titrations give a pK_a of 20.6 ± 0.2. For comparison, the protonated congener of $[Fe_2S_2Cl_4]^{2-}$ has a pK_a of 18.1 in MeCN (determined kinetically by Henderson because the protonated species is too unstable to observe).[16] That **1** is 2.5 units more basic than $[Fe_2S_2Cl_4]^{2-}$ despite having 0.2 V more positive redox potential[17] supports the suggestion that the site of protonation is different in the two clusters, N in **1** and S in $[Fe_2S_2Cl_4]^{2-}$.

Titrations of CD_3CN solutions of **4** (generated *in situ* from **2** and [DMAP-H]OTf or [pyH]OTf) with DBU (pK_a = 24.31 in MeCN)[18] were monitored by ^{1}H NMR spectroscopy (see SI). Assuming mass balance, integration of the Ar*H* resonance of **2** at 12.16 ppm gives the relative amounts of **2** and (NMR silent) **4**. A pK_a of 24.7 ± 0.4 was obtained for **4**.

Cyclic voltammograms (CVs) of **1** or **2** show two electrochemically reversible couples at −1.225 (±0.003) and −2.198 (±0.008) V versus Fc/Fc$^+$ (Figures 3b and S18). These correspond to the $Fe^{III}_2/Fe^{III/II}_2$ and $Fe^{III/II}_2/Fe^{II}_2$ couples, respectively. The large 0.973 V separation between the two couples is consistent with the observed stability of **2** toward redox disproportionation.

In contrast, the CVs of **4** and **3** show several redox events (Figures 3b and S20). This behavior is not due to species degradation, as addition of base regenerates the CVs of **2** and **1**. Additionally, CVs recorded at −20 °C are qualitatively similar to those obtained at room temperature. In the region of the $Fe^{III}_2/Fe^{III/II}_2$ couple, the CV of **4** features two broad redox events that are anodically shifted relative to that of **2**. The first wave, assigned to the **3**/**4** couple, is estimated to be −0.98 ± 0.02 V (from the shift in the oxidation peak of **2** in the presence of 1 equiv [pyH]OTf, see SI). The more anodic wave, at ∼−0.6 V, likely corresponds to the couple of a doubly protonated cluster (see SI).

The thermochemistry of interconversion of the cluster congeners is summarized in Scheme 1. The measured change in pK_a upon reduction corresponds to a free energy change of 5.6 ± 0.4 kcal mol^{-1}, and is in excellent agreement with the measured change in $E_{1/2}$ upon protonation (5.65 ± 0.10 kcal mol^{-1}), which must be equal by Hess's Law.[19] These changes are also in accord with those observed in biological Rieske clusters. For example, a change in pK_a of 6.6 ± 0.4 kcal mol^{-1} is observed upon reduction of the Rieske cluster from the cytochrome bc_1 complex of *Rhodobacter sphaeroides* (*Rs*Rp).[4a] This similar extent of thermodynamic coupling in the two systems suggests that the site of protonation is similar in both clusters.

The bond dissociation free energy (BDFE) of the NH bond of **4** is 60.5 ± 1.0 kcal mol^{-1}, as defined by the pK_a and $E_{1/2}$ values (BDFE = 23.06$E_{1/2}$ + 1.37pK_a + C_G; C_G = 54.9 ± 1.0 kcal mol^{-1} in MeCN).[19] This BDFE is 14.6 kcal mol^{-1} less than that of *Rs*Rp (75.1 ± 1.0 kcal mol^{-1}).[4a,19] Compounds **1**−**4** are thus a reasonable model for Rieske clusters in terms of the thermodynamic coupling mentioned above, but are substantially more reducing than the biological systems (**4** is a better H-atom donor). This is perhaps due to the presence of three anionic ligands in **4** versus two anionic ligands in the mixed-valence biological Rieske congener (both His ligands are protonated in the mixed-valence state). This discrepancy could also be due to the differences in the ligand type: benzimidazolate in **4** and imidazolate/thiolate in Rieske clusters.

The relatively weak BDFE indicates that H-atom abstraction from **4** should be facile. Indeed, *in situ* generated **4** reacts quantitatively with 1 equiv of the nitroxyl radical TEMPO to generate oxidized and deprotonated **1** plus 1 equiv TEMPO-H, as ascertained by NMR spectroscopy (eq 1; $\widehat{NN}$ = ^{Pr}bbim^{2-}; Figure S15).

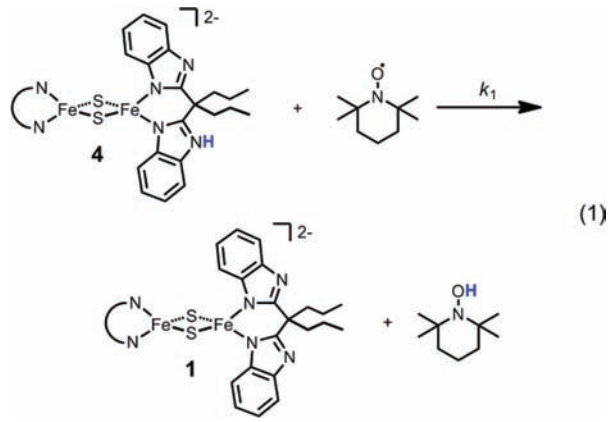

(1)

To gain insight into the mechanism of reaction 1, double-mixing stopped-flow kinetic measurements in MeCN were undertaken, under pseudo-first-order conditions of excess TEMPO (Figures S22−S23). Solutions of **2** (0.74 mM) and [DMAP-H]OTf (0.69 mM) were mixed to generate **4** *in situ*, and after a delay time of 10 s, **4** was mixed with TEMPO (3.2−8.5 mM). At 25 °C, a rate constant of 2200 ± 350 M^{-1} s^{-1} was obtained, equivalent to $\Delta G^{\ddagger}$ = 12.9 ± 0.3 kcal mol^{-1}. The temperature dependence of k_1 (−25 to 50 °C) gives $\Delta S^{\ddagger}_1$ = −38 ± 2.4 cal K^{-1} mol^{-1} and $\Delta H^{\ddagger}_1$ = 1.6 ± 0.3 kcal mol^{-1}. These values are similar to those obtained for the PCET reaction between monomeric and high-spin $Fe(H_2bim)_3^{2+}$ and TEMPO (H_2bim = 2,2′-bi-2-imidazoline).[20]

The rate constant and thermochemical data indicate that the TEMPO reaction proceeds by concerted transfer of the e$^-$ and H$^+$ (called CPET or H-atom transfer, HAT).[19] The free energy of this step, from the BDFEs of **4** (see above) and of TEMPO-H,[19] is ΔG°_{CPET} = −6.0 kcal mol^{-1}. The alternative stepwise pathways of initial ET followed by PT (with **3** + TEMPO$^-$ as intermediates) or PT followed by ET (via **2** + TEMPO-H$^{\bullet+}$), have very unfavorable free energies associated with the initial steps: ΔG°_{ET} = +22.4 kcal mol^{-1}; ΔG°_{PT} = +22.3 kcal mol^{-1}. Since these free energies are both much larger than the measured free energy barrier ($\Delta G^{\ddagger}_1$ = 12.9 ± 0.3 kcal mol^{-1}), these pathways are ruled out. As further evidence against initial ET, TEMPO is unreactive with **2** in CD_3CN, even though **2** is a

dx.doi.org/10.1021/ja3019324 | *J. Am. Chem. Soc.* 2012, 134, 7293−7296

better outer-sphere reductant than **4** ($\Delta G^{\circ}_{ET(2+TEMPO)}$ = +16.7 kcal mol^{-1}).

Complex **4** also reacts quantitatively with 0.5 equiv of 2,5-di^{t}butyl-*p*-benzoquinone (^{t}Bu$_2$Q) to give **1** and 2,5-di^{t}butyl-*p*-hydroquinone (^{t}Bu$_2$H$_2$Q) (eq 2 and Figure 1). Similar

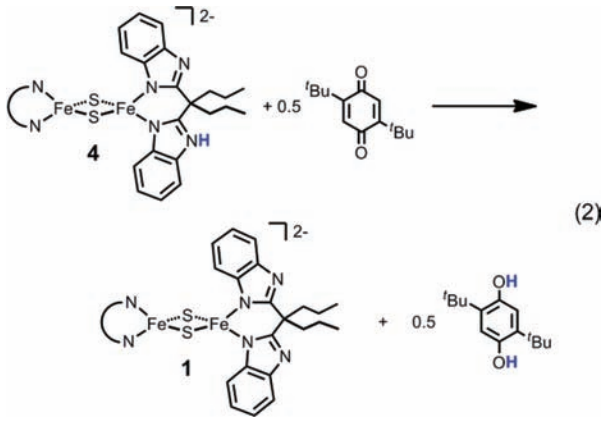

reactivity is also observed with duraquinone and ubiquinone. Hydro-ubiquinone is the biological reactant for the Rieske cluster in the mitochondrial bc_1 complex Q-cycle. Because of the difference in BDFEs, the biological reaction runs in the opposite direction, the Rieske cluster oxidizing the hydroquinone to the semiquinone radical.[4b,7] Mechanistic studies of quinone reactions are in progress. These are mechanistically complex as they are 2e$^-$/2H$^+$ reductions that proceed via the anionic and/or neutral semiquinone, SQ$^{\bullet-}$/HSQ$^{\bullet}$. Preliminary results indicate that **4** reacts with [^{t}Bu$_2$SQ$^{\bullet-}$]Na(15-crown-5) to give mixtures of **1** (45%) and **2** (55%). The semiquinone anion has been observed spectroscopically in the bc_1 complex (albeit under conditions that favor superoxide formation),[8b] and thus, it may be a relevant species in the H-atom transfer to the Rieske cluster.

In sum, we have prepared and characterized all four congeners of a bis-benzimidazolate ligated [2Fe−2S] cluster system which serves as a Rieske cluster model. The ability to prepare the protonated derivatives **3** and **4** allows for the complete thermochemical properties of the system to be established, including pK_a values for the diferric and ferric/ferrous [Fe−S] clusters. Though the BDFE of **4** is ca. 14 kcal mol^{-1} less than that observed at biological clusters, a similar degree of thermodynamic coupling is observed. Mixed-valence and protonated **4** undergoes concerted proton−electron transfer with TEMPO to give oxidized and deprotonated **1**, the first example of CPET involving a ferrous/ferric [Fe−S] cluster. Cluster **4** also reacts with quinones to give **1**. The latter is the microscopic reverse of the proposed first step in the mitochondrial Q-cycle.

■ ASSOCIATED CONTENT

Ⓢ Supporting Information

Experimental procedures and characterization data are available (.pdf), as well as crystallographic details for **1** and **2** (.cif). This material is available free of charge via the Internet at http://pubs.acs.org.

■ AUTHOR INFORMATION

Corresponding Author

mayer@chem.washington.edu

Notes

The authors declare no competing financial interest.

■ ACKNOWLEDGMENTS

We gratefully acknowledge financial support from the U.S. National Institute of Health (R01GM50422 to J.M.M. and 1F32GM099316 to C.T.S.). We thank Prof. Stefan Stoll for help with EPR experiments.

■ REFERENCES

(1) (a) Lippard, S. J.; Berg, J. M., *Principles of Bioinorganic Chemistry*; University Science Books: Mill Valley, CA, 1994; (b) Beinert, H.; Holm, R. H.; Münck, E. *Science* **1997**, *277*, 653.

(2) (a) Zu, Y.; Fee, J. A.; Hirst, J. *J. Am. Chem. Soc.* **2001**, *123*, 9906. (b) Bak, D. W.; Zuris, J. A.; Paddock, M. L.; Jennings, P. A.; Elliott, S. J. *Biochemistry* **2009**, *48*, 10193. (c) Camba, R.; Jung, Y.-S.; Hunsicker-Wang, L. M.; Burgess, B. K.; Stout, C. D.; Hirst, J.; Armstrong, F. A. *Biochemistry* **2003**, *42*, 10589. (d) Lanzilotta, W. N.; Christiansen, J.; Dean, D. R.; Seefeldt, L. C. *Biochemistry* **1998**, *37*, 11376.

(3) (a) Franz, J. A.; Lee, S.-J.; Bowden, T. A.; Alnajjar, M. S.; Appel, A. M.; Birnbaum, J. C.; Bitterwolf, T. E.; Dupuis, M. *J. Am. Chem. Soc.* **2009**, *131*, 15212. (b) Olsen, M. T.; Rauchfuss, T. B.; Wilson, S. R. *J. Am. Chem. Soc.* **2010**, *132*, 17733.

(4) (a) Zu, Y.; Couture, M. M. J.; Kolling, D. R. J.; Crofts, A. R.; Eltis, L. D.; Fee, J. A.; Hirst, J. *Biochemistry* **2003**, *42*, 12400. (b) Hsueh, K.-L.; Westler, W. M.; Markley, J. L. *J. Am. Chem. Soc.* **2010**, *132*, 7908.

(5) Ferraro, D. J.; Gakhar, L.; Ramaswamy, S. *Biochem. Biophys. Res. Commun.* **2005**, *338*, 175.

(6) (a) Osyczka, A.; Moser, C. C.; Dutton, P. L. *Trends Biochem. Sci.* **2005**, *30*, 176. (b) Berry, E. A.; Guergova-Kuras, M.; Huang, L.-S.; Crofts, A. R. *Annu. Rev. Biochem.* **2000**, *69*, 1005.

(7) (a) Lhee, S.; Kolling, D. R. J.; Nair, S. K.; Dikanov, S. A.; Crofts, A. R. *J. Biol. Chem.* **2010**, *285*, 9233. (b) Cape, J. L.; Bowman, M. K.; Kramer, D. M. *J. Am. Chem. Soc.* **2005**, *127*, 4208.

(8) (a) Cape, J. L.; Aidasani, D.; Kramer, D. M.; Bowman, M. K. *Biochemistry* **2009**, *48*, 10716. (b) Cape, J. L.; Bowman, M. K.; Kramer, D. M. *Proc. Natl. Acad. Sci. U.S.A.* **2007**, *104*, 7887.

(9) (a) Tanaka, K.; Moriya, M.; Tanaka, T. *Inorg. Chem.* **1986**, *25*, 835. (b) Henderson, R. A. *Coord. Chem. Rev.* **2005**, *249*, 1841.

(10) (a) Beardwood, P.; Gibson, J. F. *J. Chem. Soc., Chem. Commun.* **1986**, 490. (b) Beardwood, P.; Gibson, J. F. *J. Chem. Soc., Dalton Trans.* **1992**, 2457. (c) Ding, X. Q.; Bill, E.; Trautwein, A. X.; Winkler, H.; Kostikas, A.; Papaefthymiou, V.; Simopoulos, A.; Beardwood, P.; Gibson, J. F. *J. Chem. Phys.* **1993**, *99*, 6421.

(11) Albers, A.; Demeshko, S.; Dechert, S.; Bill, E.; Bothe, E.; Meyer, F. *Angew. Chem., Int. Ed.* **2011**, *50*, 9191.

(12) Rao, P. V.; Holm, R. H. *Chem. Rev.* **2004**, *104*, 527.

(13) Bertini, I.; Luchinat, C.; Parigi, G., *Solution NMR of Paramagnetic Molecules Applications to Metallobiomolecules and Models*; Elsevier: Amsterdam, 2001; Vol. 2.

(14) Beardwood, P.; Gibson, J. F.; Bertrand, P.; Gayda, J.-P. *Biochim. Biophys. Acta, Protein Struct. Mol. Enzymol.* **1983**, *742*, 426.

(15) Izutsu, K. *Acid-Base Dissociation Constants in Dipolar Aprotic Solvents*; Blackwell Scientific Publications: Oxford, 1990.

(16) Bates, K.; Garrett, B.; Henderson, R. A. *Inorg. Chem.* **2007**, *46*, 11145.

(17) Wong, G. B.; Bobrik, M. A.; Holm, R. H. *Inorg. Chem.* **1978**, *17*, 578.

(18) Kaljurand, I.; Kütt, A.; Sooväli, L.; Rodima, T.; Mäemets, V.; Leito, I.; Koppel, I. A. *J. Org. Chem.* **2005**, *70*, 1019.

(19) Warren, J. J.; Tronic, T. A.; Mayer, J. M. *Chem. Rev.* **2010**, *110*, 6961.

(20) Mader, E. A.; Davidson, E. R.; Mayer, J. M. *J. Am. Chem. Soc.* **2007**, *129*, 5153.